13th International Brick and
Block Masonry Conference
Amsterdam, July 4-7, 2004

STATIC CYCLIC TESTS ON URM WALL BEFORE AND AFTER RETROFITTING WITH COMPOSITES

M. ElGawady[1], J. Hegner[2], P. Lestuzzi[3], M. Badoux[4]

Abstract

Four years ago, an extensive experimental program for retrofitting of unreinforced masonry (URM) walls has been switched on in Switzerland. The program includes in-plane dynamic and static cyclic tests on URM walls retrofitted using composites as well as shotcrete. This paper presents preliminary test results of the static cyclic tests. The test specimens are half-scale specimens built using half-scale hollow clay masonry units and weak mortar. The specimens, before and after retrofitting, are subjected to a series of force and displacement control test runs. The test shows that the composites improve the cracking and ultimate load of the retrofitted specimen by a factor of 3 and 1.5, respectively.

Key Words

Seismic, in-plane, composites, retrofitting.

1 Introduction

Recent earthquakes have shown that many unreinforced masonry (URM) buildings are seismically vulnerable; therefore, the demand for retrofitting strategies of these buildings has become increasingly stronger in the last few years. Numerous conventional techniques have been applied for retrofitting of existing masonry buildings. Potential disadvantages of these techniques (e.g. heavy mass, limited efficiency, etc.) have been reported (e.g. ElGawady et al. 2004b, Hamid et al. 1994).
Modern composite materials offer promising retrofitting possibilities for masonry buildings. Several researchers (e.g. Holberg and Hamilton 2002, Albert et al. 2001, Ehsani et al. 1999, Schwegler 1994) explored the improvement in the ultimate in-plane and out-of-plane resistance of URM walls retrofitted with composites. A literature review of retrofitting URM walls using composites is presented in ElGawady et al. 2004a.

[1] Ph.D. Candidate, ENAC-IS-IMAC, Swiss Federal Institute of Technology Lausanne (EPFL), Switzerland, mohamed.elgwady@epfl.ch
[2] Former master student, ENAC-IS-IMAC, EPFL, Switzerland
[3] Lecturer, ENAC-IS-IMAC, EPFL, Switzerland, pierino.lestuzzi@epfl.ch
[4] Former professor, ENAC-IS-BETON, EPFL, marc.badoux@epfl.ch

One of the pioneer dynamic in-plane investigations was carried out by (ElGawady et al. 2003). The extensive study includes several test parameters: aspect ratio (slender and squat), fiber type, fiber structure, retrofitting configuration, and mortar compressive strength. The study shows that composites could increase the in-plane ultimate resistance by a factor of three. However, for squat specimens the test was stopped before the ultimate resistance of the specimens was reached. As the ultimate resistance of the retrofitted squat specimens were higher than the force capacity of the shaking table hydraulic jack. A second phase of the project, including static cyclic tests on eleven squat specimens with two aspect ratios (0.67, 0.50), was carried out. Finally, the experimental results of the modern retrofitting fiber reinforced plastic "FRP" are compared to experimental results of a classical retrofitting scheme "shotcrete".

2 Experimental program

The experimental results presented here are part of the ongoing static cyclic testing program. This paper reports on the following two tests:

- S2-REFE-ST: reference test on an unreinforced masonry wall
- S2-WRAP-G-F-ST: test on the S2-REFE-ST specimen after retrofitting on one face with one layer of glass FRP (GFRP)

2.1 Description and construction of the test specimens

The test specimens are representative of an unreinforced clay masonry wall in the upper floors of a typical Swiss building of the 1950's. Half-scale squat masonry walls were built by experienced masons using half-scale hollow clay masonry (HCM). The walls were constructed in a single wythe, in a running bond pattern with a mortar joint of 5 mm thickness, which is consistent with the half scaled bricks. The nominal dimensions of the walls are 710 mm height, 1570 mm length, and 75 mm width. Both the head beam and foundation pad were pre-cast concrete. The main geometric features of the constructed walls are illustrated in Figure 1.

2.1.1 Bricks and mortar

The original HCM unit is 300 X 150 X 190 mm; this resulted in a scaled brick nominally measuring 150 X 75 X 95 mm. A commercial firm produced the scaled HCM units. The specimens were built using a weak mortar with an average compressive strength of 3.2 MPa and a standard deviation of 0.35 MPa.

2.1.2 Upgrading procedure

After testing specimen S2-REFE-ST until failure, the specimen was retrofitted using a layer of bidirectional glass fiber (SikaWrap-300G 0/90). Table 1 gives the fiber characteristics according to manufacture's data. The composites were applied on one face of the masonry wall using two-component epoxy Sikadur-330.

The application of the wrap material was a simple and rapid operation. The surface was roughened by grinding, cleaned with high air pressure. It was then coated with a thin layer of Sikadur-330. To ensure that anchorage failure did not occur, steel plates were used to anchor the GFRP to the r.c. head beam and foundation pad.

Table 1 GFRP Characteristics

Commercial name	FRP [Fiber]	$Warp_W$ [g/m^2]	$Weft_W$ [g/m^2]	f_t [MPa]	E [GPa]	ε [%]
SikaWrap-300G 0/90	Glass	145	145	2400	70	3.0

$Warp_w$ and $Weft_w$: Weight of fiber in the warp and weft directions respectively

f_t , E, and ε: Fibers nominal tensile strength, Young's modulus, and ultimate strain respectively

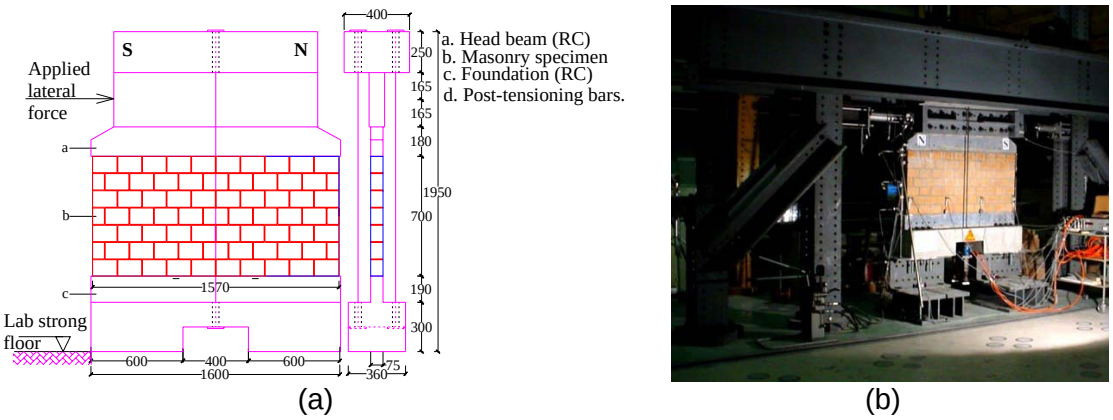

(a) (b)

Figure 1 Specimen (a) dimensions [mm], and (b) ready to test

2.2 Test set-up and loading system

A test specimen was constructed on a precast r.c. footing, which was post-tensioned to the laboratory strong floor (Figure 2). After allowing the specimen to cure (from 3-7 days), the head beam was fixed to the top of the specimen using strong mortar (M20). Superimposed gravity load of approximately 30 kN was simulated using two external post-tensioning bars. This was in addition to 12 kN of self-weight from steel elements at wall top (due to the test set-up), r.c. head beam, and masonry panel weight. This normal force corresponds to a stress of 0.35 MPa. Railcar springs were used with the post-tensioning bars to avoid increment in the post-tensioning force due to bars elongation. The post-tensioning bars elongate due to the increment in the specimen height because of flexural cracks opening.

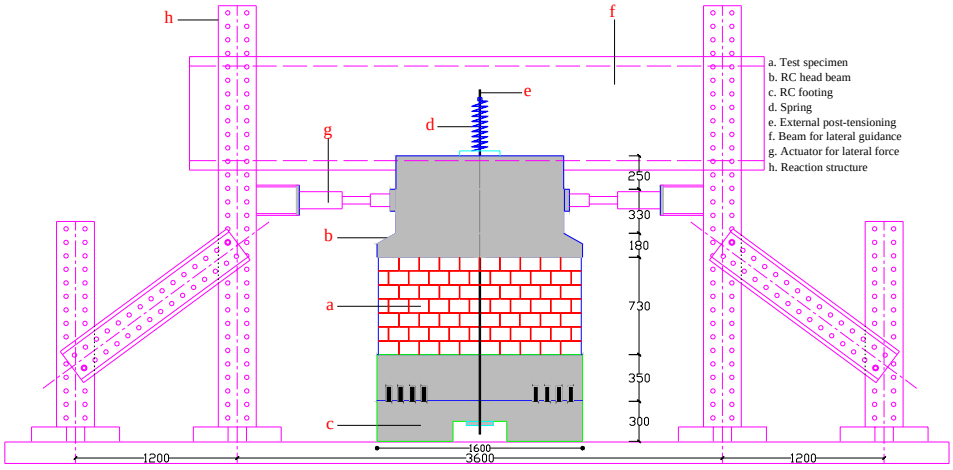

Figure 2 Test set-up [mm]

The horizontal load was applied to the reinforced concrete head beam, which in turn distributes the force to the masonry wall. The load was applied manually using two hydraulic jacks and hand pumps. The specimens can be considered cantilever walls, i.e. fixed at the base and free at the top with an effective aspect ratio of 0.67 (height of the horizontal force above the base of the masonry wall of 1.00 m and width of 1.6 m).
The specimens were subjected to a sequence of test runs (Figure 3): each test run is a half cycle. Before cracking (force control), the applied force was increased gradually with increment of approximately 5 kN. At each applied load, the specimens were subjected to complete cycle (i.e. two successive test runs). After cracking (displacement control), the first ram (test run in the cracked direction) was controlled by a predefined sequence of displacements (Figure 3), while in the other direction (i.e.

next test run or half cycle) the test was controlled in accordance with the measured forces in the previous test run. In this way, equal forces were applied on both sides of a wall specimen. This is related well to what observed during real time dynamic test (ElGawady et al. 2003).
The predefined sequence of displacements was similar to that proposed in the ICBO (1997). At first cracking, the measured relative displacement at wall top was used to mark the "first yield displacement". As shown in Figure 3, at each ductility level the specimens were subjected to three complete cycles.

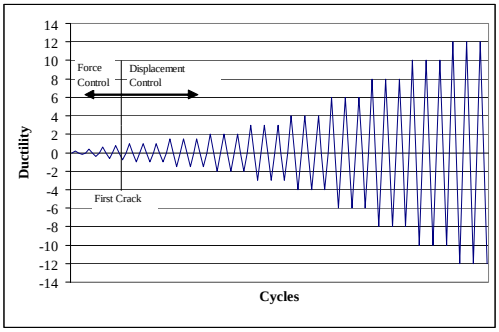

Figure 3 Loading sequence

2.2.1 Instrumentation

The specimens were instrumented with several devices as shown in Figure 4. Seventeen Linear Variable Displacement Transducers (LVDTs) measured vertical, horizontal, and diagonal displacements and deformations. The horizontal strains in the FRP were measured using electrical strain gages (Figure 4(b)). The forces in the post-tensioning bars as well as the lateral forces at the wall top were measured using four load cells.

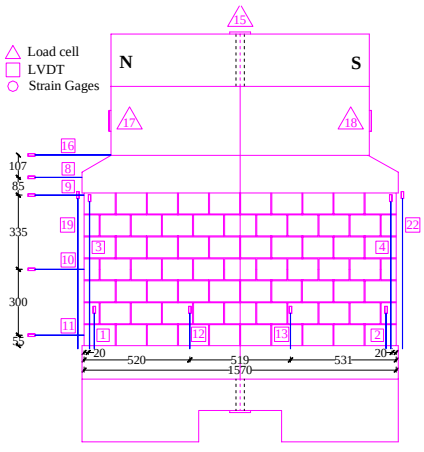

(a)

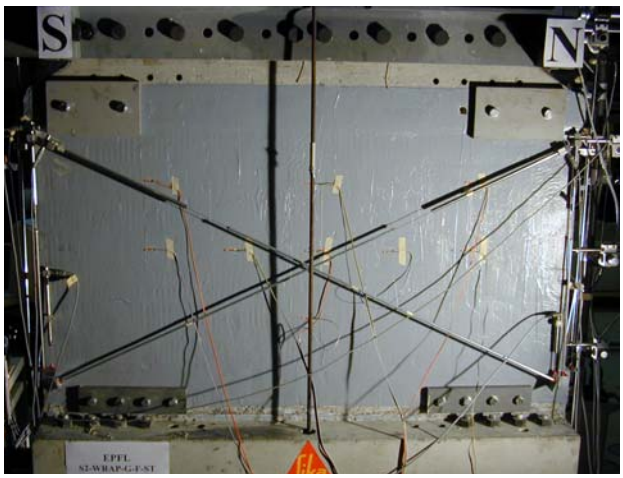

(b)

Figure 4 Specimen S2-WRAP-G-F-ST instrumentations on the (a) western face and (b) eastern (retrofitted) face

2.3 Test results

Table 2 presents a summary of the test procedure, the measured lateral forces, and drifts for selected test runs. Figure 5 to Figure 7 show the observed damage to the test specimens during and at the test end. In order to determine sliding between the masonry panel and the r.c. foundation, Figure 8 shows a comparison between the total displacement (i.e. the relative displacement between the wall top and foundation pad) and the relative displacement between wall top and the first brick course. The vertical

axis in the figure is the lateral load at the specimen top. This figure is presented for selected cycles only. Figure 5 to Figure 8 and Table 2 are complemented by the following comments regarding the specimen behavior during the tests.

2.3.1 Specimen S2-REFE

- During test run 5, a first flexural crack formed in the first bed joint (i.e. between the masonry panel and the foundation pad) at northern side. The crack propagated towards southern side (Figure 6 (a)) during subsequent test runs.
- During test run 30, a first flexural crack formed in the second bed joint at southern side (Figure 9(a)). The crack propagated towards northern side during subsequent test runs (Figure 6 (b)).
- During test runs 45 to 52, a significant flexural crack (Figure 6(c)) extended between the fourth and third bed joints happened.
- During test run 65, the specimen displayed a characteristic rocking (Figure 9(b)) and a first toe vertical compressive crack happened in the southern side.
- During test runs 66 and 67, sliding occurred with deformation concentrated through the first bed joint. The sliding was about 1 mm in the south-north direction and 2.5 mm in the north-south direction (Figure 8(a)).

Table 2 Loading history and main test results for test specimens

North-south direction						South-north direction					
Run	Control	Target	P [kN]	F [kN]	Drift [%]	Run	Control	Target	P [kN]	F [kN]	Drift [%]
S2-REFE											
5	F.C.	15.0 kN	30.1	15.1	0.02	6	F.C.	15.0 kN	29.9	15.2	0.02
7	D.C.	Δ=1 Δ_y	30.0	14.7	0.05	8	F.C.	14.7 kN	29.9	14.9	0.02
29	D.C.	Δ=4 Δ_y	30.8	25.0	0.15	30	F.C.	25.0 kN	29.8	24.9	0.05
51	D.C.	Δ=10 Δ_y	31.4	30.8	0.35	52	F.C.	30.8 kN	29.9	30.7	0.20
63	D.C.	Δ=16 Δ_y	30.7	31.5	0.53	64	F.C.	31.5 kN	27.9	31.2	0.31
65	D.C.	Δ=20 Δ_y	33.4	**33.7**	0.70	66	D.C.	Δ=30 Δ_y	34.9	**37.3**	1.02
67	D.C.	Δ=25 Δ_y	31.8	30.8	0.69	68	D.C.	Δ=25 Δ_y	31.4	34.2	0.73
71	D.C.	Δ=35 Δ_y	34.4	27.6	1.08	72	D.C.	Δ=35 Δ_y	33.6	33.0	1.00
75	F.C.	18.0 kN	31.4	18.1	1.46						
S2-WRAP-G-F-ST											
15	F.C.	45 kN	30.2	45	0.17	16	F.C.	45 kN	30.3	45	0.16
21	D.C.	Δ=1.5	31.1	**47**	0.28	22	F.C.	47 kN	30.3	47	0.17
23	D.C.	Δ=1.5	30.9	35	0.26	24	D.C.	Δ=1.5	31.1	**55**	0.28
37	D.C.	Δ=3 Δ_y	33.0	17	0.51	38	D.C.	Δ=3 Δ_y	33.9	35	0.55
39	D.C.	Δ=4 Δ_y	33.7	17	0.56	40	D.C.	Δ=4 Δ_y	36.8	36	0.84
55	D.C.	Δ=10 Δ_y	35.3	13	1.58	56	D.C.	Δ=10 Δ_y	35.8	27	1.84
57	D.C.	Δ=14 Δ_y	30.7	11	1.91	58	D.C.	Δ=14 Δ_y	37.6	26	2.35
						59	D.C.	Δ=18 Δ_y	31.1	17	2.80

F.C., D.C.: Force control, and displacement control respectively
P., F: Measured peak post-tensioning and peak lateral forces

(a) (b)

Figure 5 Specimens (a) S2-REFE-ST and (b) S2-WRAP-G-F-ST (unreinforced face) at the test end

(a) (b) (c)

Figure 6 S2-REFE-ST (a) opening of the first crack in the northern side, (b) opening of the first crack in the southern side, and (c) opening of the crack between the third and fourth mortar joint in the northern side

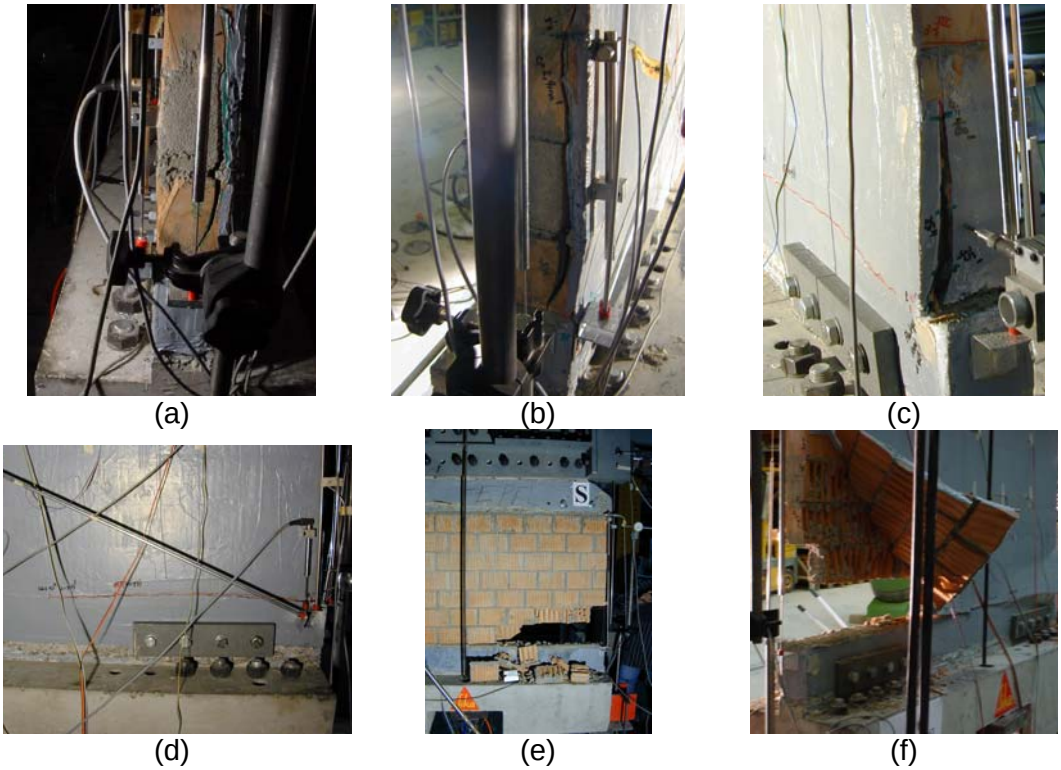

(a) (b) (c)

(d) (e) (f)

Figure 7 S2-WRAP-G-F-ST (a) opening of first crack in the southern side, (b) propagation of the first crack in the southern side, (c) vertical crack in the northern side, (d) tear of GFRP during the test, (e) rupture of GFRP at the test end, and (f) crushing of masonry at the test end

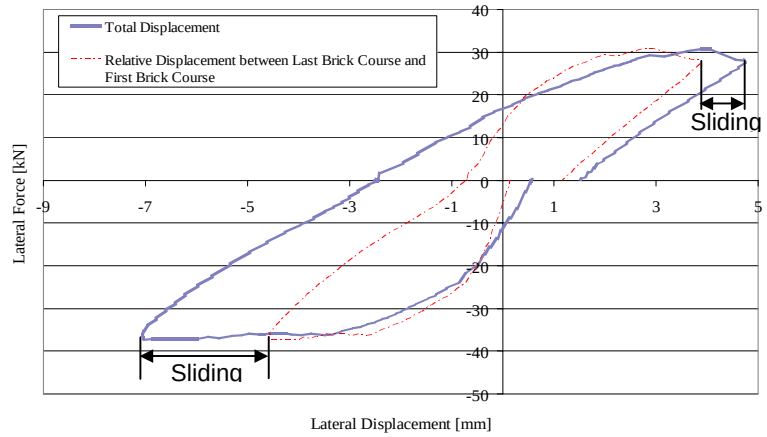

(a)

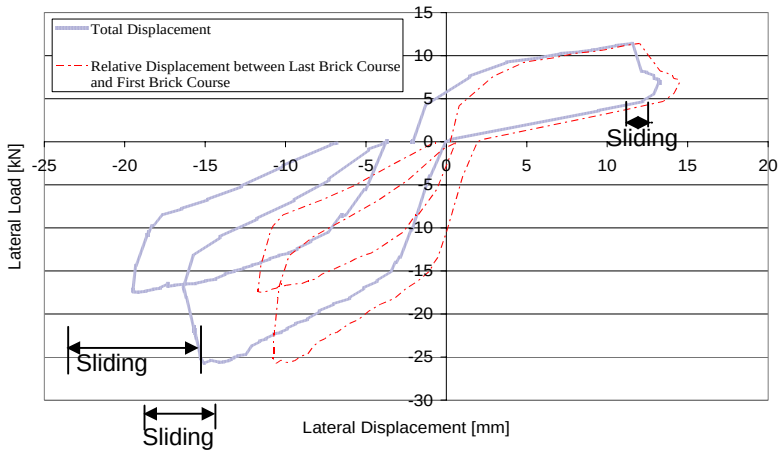

(b)

Figure 8 Measured sliding between masonry panel and r.c. foundation during test runs (a) 66, 67 for S2-REFE-ST, and (b) 57 to 59 for S2-WRAP-G-F-ST

- During test run 72, a vertical compressive crack in the northern toe happened. Then, the test was stopped towards south-north direction and continued in the other direction. After test run 75, the southern side was heavily damaged and the test was stopped.

2.3.2 Specimen S2-WRAP-G-F

- Before retrofitting of S2-REFE-ST using GFRP, new bricks replaced the three damage bricks at the southern side. However, the test results of S2-WRAP-G-F-ST influenced by the replacement of bricks as well as heavy damage of S2-REFE-ST.
- During test run 15, a vertical crack of 300 mm length happened in the substrate behind the GFRP the specimen southern side (Figure 7 (a)).
- During test run 16, a 20 mm length horizontal tear in the northern side happened in the GFRP at the first mortar joint.
- During test run 21, the tear of the GFRP extended instantaneously over 400 mm length. This tear extension combined with relatively high increment in the lateral drift (Figure 10 (a) and Table 2). In addition, the maximum lateral load in the north-south direction was recorded during this test run. In the next test runs, the tear extended gradually (Figure 7(c), (d)).
- During test run 24, a horizontal tear of approximately 400 mm length instantaneously happened in the GFRP at the level of the first mortar joint. It is

worth to note that in this test run the specimen was controlled in displacement control instead of force control. This decision was made since no cracks or GFRP rupture was observed in the specimen southern side until 47 kN (test run 22) hence it has no sense to apply a smaller force (35 kN) which was recorded during test run 23.

- During test runs 25 to 38, a vertical crack in the substrate behind the GFRP along 150 mm length was observed in the northern side (Figure 7(c)).

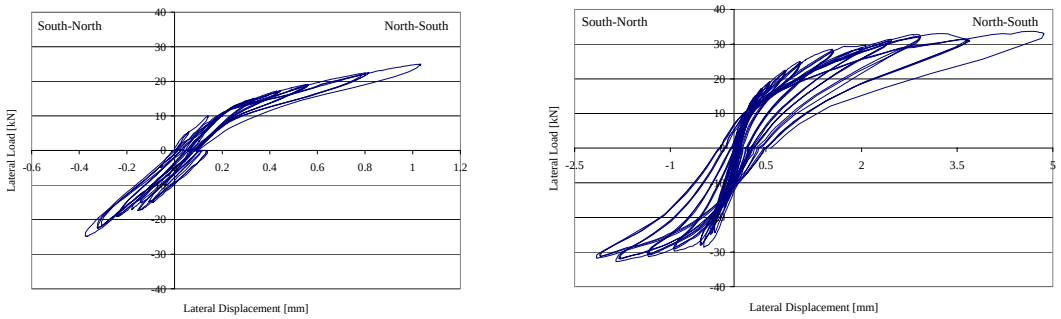

(a) (b)

Figure 9 Specimen S2-REFE-ST, lateral forces vs. relative wall displacement until (a) test run 30, and (b) test run 65

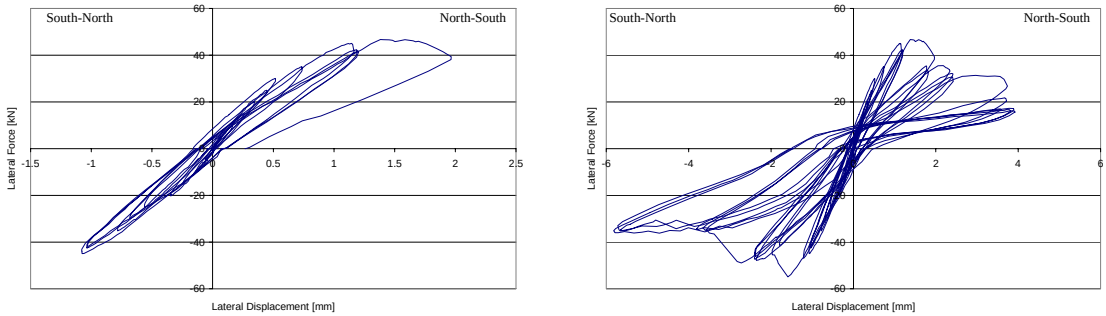

(a) (b)

Figure 10 Specimen S2-WRAP-G-F-ST, lateral forces vs. relative wall displacement until (a) test run 21, and (b) test run 44

- Initiation of delamination was observed in a few points during test runs 39 and 40. This delamination was visible in the form of white spots on the wrap.
- During test runs 39 to 56, the specimen displayed a stable rocking behavior (Figure 10(b)) with bricks in the toe and heal subjected to heavy damage. The damage propagation in the southern side was relatively unfamiliar: the damage propagated from the second to the first brick courses. This damage propagation could be an effect of brick replacement.
- During test runs 58 and 59, sliding occurred with deformation concentrated through the first bed joint (i.e. between the masonry wall and its foundation). The sliding was about 7 mm in the south-north direction and about 1mm in the north-south direction (Figure 8 (b)).
- After test runs 57 and 59, the specimen heavily damaged and the test was stopped as the lateral resistance dropped to less than 30% of the peak lateral resistance.

2.4 Comparison of test specimen S2-REFE-ST and S2-WRAP-G-F-ST

Figure 11 shows the hysteretic behavior of each test specimen. The axes are the relative horizontal displacement between the top and base of the masonry wall and the

horizontal load at top of the wall. In addition, Figure 12 shows a superposition of the backbone curves for the specimens in the north-south direction and the inverse direction. The following comments complete the comparison between the two specimens:

- Both specimens developed a rocking mode and a significant lateral deformation capacity.
- The upgrading forced a move of the "rocking crack" from 2nd and 3rd course (S2-REFE-ST) to the base of the masonry wall (S2-WRAP-G-F-ST).
- At initiation of rocking, the lateral load in S2-WRAP-G-F-ST is about 3 times that in S2-REFE-ST. However, this high improvement is due to the very weak tensile strength of masonry.
- At ultimate lateral load, the lateral resistance of S2-WRAP-G-F-ST was about 1.5 times the lateral resistance of S2-REFE-ST. This limited improvement was due to the heavy damage in the reference specimen before retrofitting.

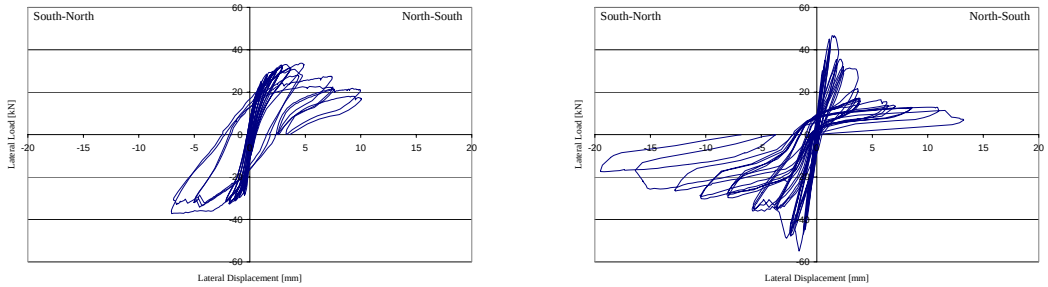

(a) (b)

Figure 11 Lateral forces vs. relative top wall displacement for (a) S2-REFE-ST, and (b) S2-WRAP-G-F-ST

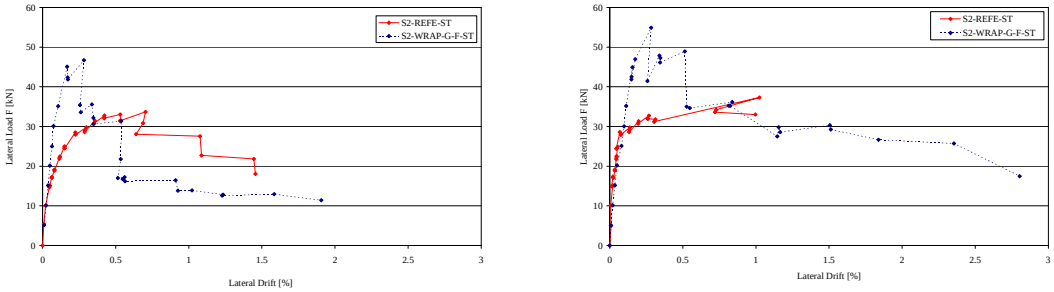

(a) (b)

Figure 12 Backbone curve for specimen S2-REFE-ST and S2-WRAP-G-F-ST (a) north-south direction, and (b) south-north direction

- After more than 30 and 20 rocking cycles for S2-REFE and S2-WRAP-G-F-ST respectively, both specimens slide over the r.c. foundation.
- During sliding, the coefficient of friction was not the same in both specimens. For S2-REFE, the coefficient of friction was approximately 1.0 while for S2-WRAP-G-F-ST was approximately 0.7. This degradation in the coefficient of friction attributed to the very heavy damage in S2-WRAP-G-F-ST.
- Although the heavy damage of specimen S2-REFE-ST at the end of the test, the retrofitting using FRP recovered the specimen initial stiffness (Figure 12).
- After GFRP rupture in the north-south direction, a high rate of the specimen lateral resistance degradation happened (Figure 12(a)). In the other loading direction, this degradation rate was smaller (Figure 12(b)). In both cases and after few cycles of GFRP rupture, the lateral resistance dropped to a value corresponding to the lateral resistance at the test end of the reference specimen.

- Although S2-WRAP-G-F-ST had a high lateral drift at the test end, no debris falls down. This preventing, in a real earthquake event, possible injury to occupants in the vicinity of a wall.

2.5 Summary

Two half-scale URM test specimens were subjected to a static cyclic loading. The first one was an unreinforced masonry specimen as a reference; the next one was retrofitted with glass fiber wrap. The tests lead to the following findings:

- The one-sided retrofitting with glass fiber wrap is promising; it improved the specimen cracking load and lateral resistance by a factor of about 3 and 1.5 respectively.
- After composite rupture, the retrofitted specimen behaved similarly to the reference specimen.
- This test confirms that wall rocking can be a stable non-linear response in unreinforced masonry walls, providing significant lateral deformation capacity.
- In spite of relatively poor mortar, the specimen friction coefficient exceeded 1.0. However, after heavy damage and a drift of approximately 2%, the specimen coefficient of friction reduced to 0.7.

Acknowledgments

The authors thank SIKA for supplying and applying the retrofitting materials as well as MORANDI for supplying the masonry bricks.

References

Albert, I. Micheal, Elwi, E. Alaa; and Cheng, J. J. Roger, (2001), “Strengthening of Unreinforced Masonry Walls Using FRPs”, J. Comp. for Constr., ASCE, Vol. 5, No. 2, 76-84.

ElGawady, M., Lestuzzi, P., Badoux, M., 2004a, A review of retrofitting of URM walls using composites, 4th Int. Conf. Adv. Comp. Mat. Bridges and Struc., Calgary, Canada

ElGawady, M., Lestuzzi, P., Badoux, M., 2004b, A review of conventional seismic retrofitting techniques for URM, 13th IB^{2}MaC, Amsterdam, Holland.

ElGawady, M., Lestuzzi, P., Badoux, M., 2003, Dynamic tests on URM walls before and after upgrading with composites, Exper. Rep., Pub. No. 1, IMAC, ENAC, EPFL, Switzerland.

ElGwady, M. A., Lestuzzi, P., Badoux, M., 2002, Dynamic in-plane behavior of URM wall upgraded with composites, 3rd ICCI’02, Ca., USA, Paper No. 009.

Hamid, A., Mahmoud, A., Abo El Maged, S., 1994, Strengthening and repair of unreinforced masonry structures: state-of-the-art, 10th IB^{2}MaC, Calgary, Canada, 485-497.

Holberg, A. M., Hamilton, H. R., 2002, Strengthening URM with GFRP composites and ductile connections.” Earth. Spec., (18) 1, 63-84.

Ehsani, M., Saadatmanesh, H., Velazquez-Dimas, J. I., 1999, Behavior of retrofitted URM walls under simulated earthquake loading, J. of Comp. for Cons., ASCE, 3(3), 134-142.

Schwegler, G., 1994, Masonry construction strengthened with fiber composites in seismically endangered zones, 10th ECEE, Vienna, Austria, 2299-2303.

International Conference of Building Officials-ICBO, 2001, Acceptance criteria for concrete and reinforced and unreinforced masonry strengthening using fiber-reinforced polymer (FRP), Composite Systems, AC125, Whittier, Ca., USA.